Biochemical and Biophysical Research Communications **257,** 168–176 (1999)
Article ID bbrc.1999.0389, available online at http://www.idealibrary.com on IDEAL®

The Influence of SV40 Immortalization of Human Fibroblasts on p53-Dependent Radiation Responses

Manu Kohli and Timothy J. Jorgensen[1]
Department of Radiation Medicine, Division of Radiation Research, Vincent T. Lombardi Cancer Center, Georgetown University Medical Center, 3970 Reservoir Road, N. W., Washington, DC 20007-2197

Received February 15, 1999

The simian virus 40 large tumor antigen (SV40 Tag) has been ascribed many functions critical to viral propagation, including binding to the mammalian tumor suppressor p53. Recent studies have demonstrated that SV40-transformed murine cells have functional p53. The status of p53 in SV40-immortalized human cells, however, has not been characterized. We have found that in response to ionizing radiation, p53-dependent p21 transactivation activity is present, albeit reduced, in SV40-immortalized cells and that this activity can be further reduced with either dominant negative p53 expression or higher SV40 Tag expression. Furthermore, overexpression of p53 in SV40-immortalized ataxia-telangiectasia (A-T) cells restores p53-dependent p21 induction to typical A-T levels. All SV40-immortalized cell lines exhibited an absence of G_1 arrest. Moreover, all SV40-immortalized cell lines exhibited increased apoptosis relative to primary cells in response to ionizing radiation, suggesting that SV40 immortalization results in a unique phenotype with regard to DNA damage responses.

Key Words: **SV40; p53; cell cycle; apoptosis; p21.**

The p53 tumor suppressor protein has been demonstrated to be activated in response to a variety of DNA damaging agents, suggesting that it plays a pivotal role in modulating the DNA damage response by providing an important link between detection of DNA damage and cell cycle control or apoptosis (1–3). Recent studies investigating DNA damage responses have shown that p53 is phosphorylated in vivo after genotoxic stress (4), thereby confirming p53's involvement in DNA damage-mediated signal transduction.

Activation of p53 results in either G_1 cell cycle arrest or apoptosis (5). The current paradigm of p53 activation maintains that p53-induced cell cycle arrest after DNA damage provides the cell with sufficient time to repair damage before DNA synthesis initiates so that heritable or potentially lethal genetic changes will not occur. If the cell is unable to repair the damage, p53-mediated apoptosis, or programmed cell death, ensues as a protective response against carcinogenesis. Growth arrest by p53 has been shown to be dependent upon p53's transcriptional activation function (6, 7). An important gene induced by p53 in response to radiation is *WAF/CIP1* (2), whose protein product, p21, binds and inactivates cyclin-dependent kinases to stall the cell cycle.

The SV40 Tag has been shown to bind to the p53 protein (8–10). The ability of the SV40 Tag to bind to p53 is required for it to extend the life span of human cells (11). This has been interpreted to mean that binding amounts to inactivation of p53 function and that SV40-immortalized cells should display an effectively p53-null phenotype. However, recent studies have demonstrated that, in SV40-transformed murine cells, p53 is still functional (12). The integrity of p53 responses in SV40-immortalized human cells, however, has not been characterized. This is an important issue, because if SV40-immortalized human cells have a p53 null phenotype, cellular responses of primary cells that are maintained following SV40-immortalization must be p53 independent.

In this study, we have investigated the functionality of p53 in SV40-immortalized human fibroblasts by examining the radiation-dependent induction of p21, a radiation response protein whose induction by ionizing radiation is known to be p53-dependent. Furthermore, two p53-mediated phenotypes, radiation-induced G_1 cell cycle arrest and apoptosis, were was also assessed

[1] To whom correspondence should be addressed at Department of Radiation Medicine, Georgetown University Medical Center, The Research Building/Room E212A, 3970 Reservoir Road, N.W., Washington, DC 20007-2197. Fax: 202-687-2221. E-mail: jorgensent@odrge.odr.georgetown.edu.

Abbreviations: A-T: ataxia-telangiectasia; DAPI: 4′,6-diamidino-2-phenylindole; DMEM: Dulbecco's Modified Eagle's Medium; EDTA: ethylenediaminetetraacetic acid; NP-40: Nonidet P-40; PBS: phosphate buffered saline; P.I.: propidium iodide; PMSF: phenylmethylsulfonyl fluoride; Rb: retinoblastoma protein; RNase: ribonuclease A; SDS: sodium dodecyl sulfate; SDS-PAGE: sodium dodecyl sulfate-polyacrylamide gel electrophoresis; SV40: simian virus 40; SV40 Tag: simian virus 40 large tumor antigen.

0006-291X/99 $30.00

in these cell lines. We demonstrate that p53-mediated p21 upregulation is still functional in SV40-immortalized fibroblasts, yet G_1 cell cycle arrest is absent. In addition, SV40 immortalization results in increased radiation-induced apoptosis.

MATERIALS AND METHODS

Cell lines and cell culture. MRC-5 primary human fetal lung fibroblasts, WI-38 primary and WI38VA13 SV40 immortalized human fetal lung fibroblasts were purchased from American Type Culture Collection (Rockville, MD). MRC-5V1 SV40 immortalized human fetal lung fibroblasts were generously provided by Dr. Colin Arlett. FT169A (AT22IJE-T) SV40 immortalized A-T fibroblasts were generously provided by Dr. Yosef Shiloh (13).

The p53 expression vectors pC53-SN3 (wild-type p53), pC53-SCX3 (dominant negative p53 with $143^{Val \rightarrow Ala}$ mutation), and the empty vector, pCMV-Neo-Bam, were generously provided by Dr. Bert Vogelstein (14). WI38VA13 pCMV-Neo-Bam and WI38VA13 pC53-SCX3 cell lines were generated by transfecting pCMV-Neo-Bam and pC53-SCX3, respectively, into WI38VA13 cells using the Lipofectin (Life Technologies; Gaithersburg, MD) stable transfection protocol. Briefly, 20 μg of above plasmids were transfected into WI38VA13 cells. The cells were allowed to grow for 48 h in growth medium and were subsequently subcultured in medium containing 1 mg/ml G418 (Life Technologies; Gaithersburg, MD) to isolate clones. FT169A pC53-SN3, FT169A pC53-SCX3, and FT169A pCMV-Neo-Bam cell lines were developed as described above by transfecting the appropriate vector into FT169A A-T fibroblasts.

WI38VA13, FT169A, MRC-5, and MRC-5V1 cells were maintained in DMEM supplemented with 10% fetal bovine serum, 2x glutamine (Biofluids, Inc.; Rockville, MD), and 100 U/ml penicillin and 100 μg/ml streptomycin (Life Technologies; Gaithersburg, MD). The WI38VA13 and FT169A transfectants were maintained in the above medium supplemented with 1 mg/ml G418. Cells were maintained at 37°C in a humidified atmosphere containing 5% CO_2.

Western blotting. For Western analysis, 5×10^5 cells were plated in 25-cm^2 flasks and allowed to grow for 48 h before irradiating with a ^{137}Cs Shepherd Mark I Irradiator. Cells were harvested at the appropriate time points by washing twice in PBS (Life Technologies; Gaithersburg, MD), scraping the cells into PBS using a cell scraper, and pelleting at 1,000 $\times$ g. The cell pellets were lysed using 50 μL cell lysis buffer (25 mM Tris pH 7.4, 50 mM NaCl, 0.5% Na deoxycholate, 2% NP-40, 0.2% SDS, 1 mM PMSF, 50 μg/ml aprotinin, 50 μM leupeptin) by incubating on ice for 15 min with vortexing every 5 min. Cell debris was removed by centrifuging the lysate at 16,000 $\times$ g for 15 min at 4°C. 2 μL of the supernatant was used to determine the protein concentration using the Bio-Rad Protein Assay (Bio-Rad Laboratories; Hercules, CA). The remainder of the sample was prepared for gel electrophoresis. 5 μL 5x SDS-PAGE loading buffer (Bio-Rad) was added to each tube and the samples were boiled for 5 min. 10–20 μg protein was loaded per lane on 12% SDS-PAGE discontinuous gels, and the samples were electrophoresed at 200 V for 45 min in the Bio-Rad Mini PROTEAN II (Bio-Rad) apparatus. The electrophoresed proteins were subsequently transferred to 0.2 μm nitrocellulose membranes (Bio-Rad) using the Bio-Rad Mini Trans-Blot apparatus.

Membranes were probed with the appropriate primary antibodies, and proteins were detected with the ECL or ECL Plus Western Blotting systems (Amersham; Arlington Heights, IL). The primary antibodies used were as follows: anti-p53 (Santa Cruz Biotechnology; Santa Cruz, CA; DO-1, 1 μg/ml); anti-p21 (Oncogene Research Products; Cambridge, MA; Ab-1, 1 μg/ml); anti-GAPDH (Trevigen; Gaithersburg, MD; 1:4000 dilution, rabbit polyclonal); and anti-SV40 large T antigen (Santa Cruz; Pab 101, 1 μg/ml).

Densitometry. Densitometric analysis of the Western blots was performed by using Scion Image densitometry software (Scion Corporation; Frederick, MD). For p21 immunoblots, band intensities were normalized to the 10 Gy irradiated 0 h p21 bands to determine fold induction of p21 protein post-irradiation. For the SV40 Tag immunoblots, SV40 Tag band intensities were normalized to the WI38VA13 SV40 Tag bands to determine the relative levels of SV40 Tag protein between WI38VA13 and the appropriate cell line.

Cell cycle analysis. For cell cycle analysis, 1×10^6 cells were plated in 175-cm^2 flasks and allowed to grow for 48 h. The cells were irradiated with the Mark I irradiator and harvested by trypsinization. Cells were fixed with 70% ethanol, washed twice in PBS, and treated with 2 ml RNase solution (100 μg/ml RNase, 0.1% Triton X-100, 0.1 mM EDTA, in PBS) at 37°C for 30 min. Subsequently, 25-50 μg/ml of P.I. solution (0.5 ml P.I. stock solution (5 mg/ml) in 50 ml RNase working solution, or 10 μL stock in 1 ml RNase solution) was added and incubated at 37°C for 30 min, then 4°C for 1 h. Cell cycle analysis was performed by the FACSort instrument, and DNA histograms were generated with Modfit software (Verity Software House, Inc.).

Apoptosis assay. To measure apoptosis, 1×10^5 cells were plated in 35 mm petri dishes and allowed to grow for 24 h. The media was exchanged with fresh media (to remove floating cells that were killed through plating effects rather than as a result of treatment) immediately prior to irradiation. The cells were irradiated with the Mark I irradiator and processed. Apoptosis was determined by collecting all floating cells in the media and combining them with the adherent cells that were harvested by trypsinization. The cells were pelleted at 1000 x g, fixed in 10% neutral buffered formalin (Sigma; St. Louis, MO) for 10 min, then resuspended in a suitable volume of 50% glycerol/PBS solution containing 80 ng/ml DAPI (Molecular Probes, Inc.; Eugene, OR). 5–10 μl of this solution was placed on a glass slide with coverslip and viewed using fluorescence microscopy with an excitation wavelength of 358 nm. Approximately 500 cells were counted for each cell line per time point, and the apoptotic index was determined by dividing the number of apoptotic cells (identified by chromatin condensation) by the total number of cells counted.

RESULTS

p53-dependent p21 protein induction in SV40 immortalized human fibroblasts. Our initial studies of p53 activity involved measuring p53 protein levels by immunoblotting. All SV40-immortalized cell lines, however, showed elevated p53 levels (data not shown) which rendered the measurement of p53 protein induction post-irradiation extremely difficult against an extremely high un-induced background. Thus, it appeared more constructive to determine p53 activity through measurement of p53-dependent p21 transactivation. In order to study p53-mediated transactivation of p21 following DNA damage, logarithmically growing cells were irradiated with 10 Gy of ionizing radiation and harvested at 0, 3, 6, 9, 12, and 24 h post-irradiation. Unirradiated cells were also harvested at 12 and 24 h as controls. Various wild-type and recombinant lines were compared. Immunoblotting of protein lysates for p21 showed that primary WI-38 cells had good induction of p21 post-irradiation (Figure 1A), whereas SV40 immortalized WI-38 cells (WI38VA13) had reduced p21 induction (Figure 1B). Expression of dominant negative p53 in WI38VA13 fibroblasts further reduced p21 induction (Figure 1D)

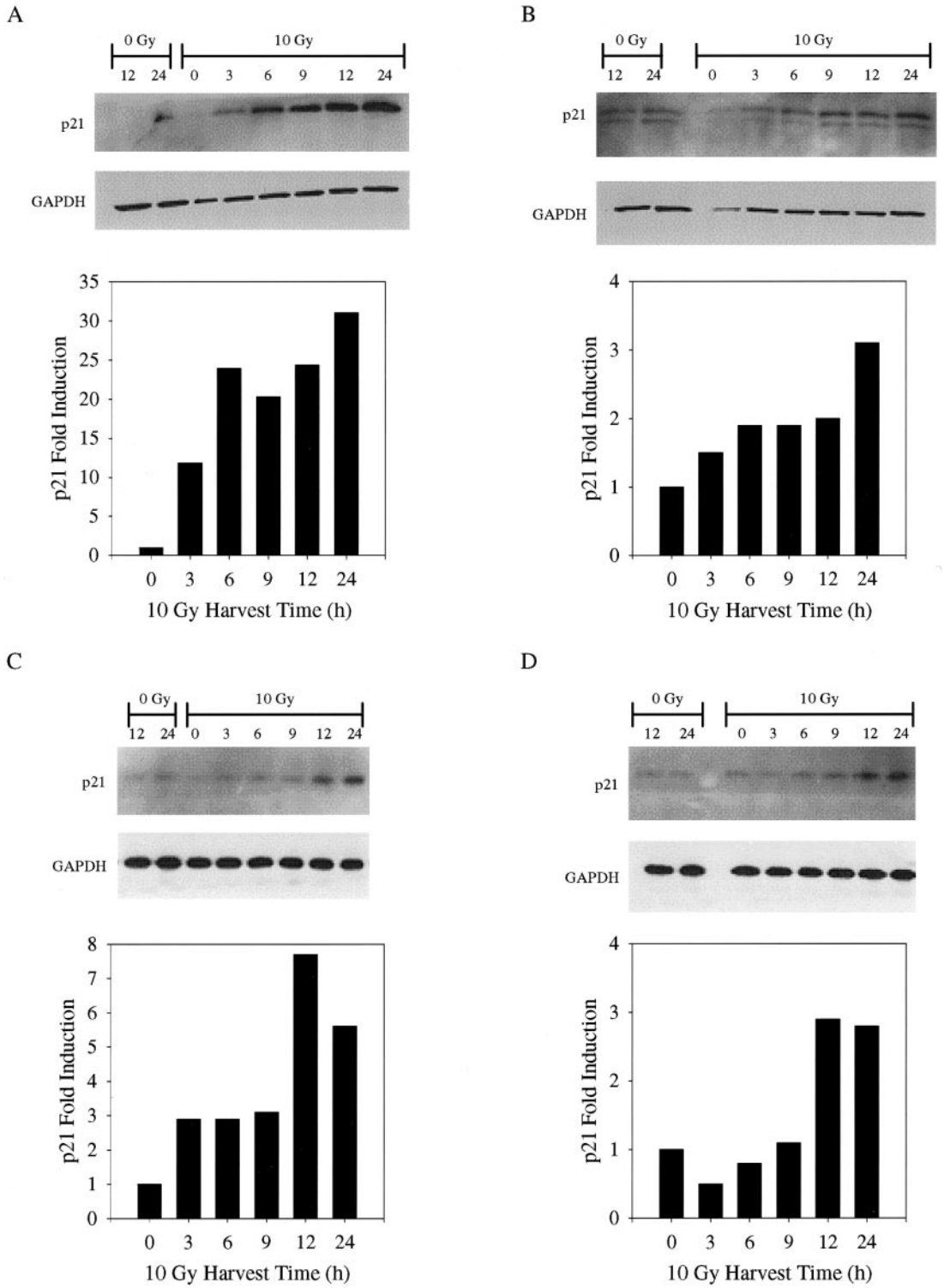

FIG. 1. Western blot showing p53-dependent p21 induction following 10 Gy ionizing radiation in A) WI-38, B) WI38VA13, C) WI38VA13 pCMV-Neo-Bam empty vector, and D) WI38VA13 pC53-SCX3 dominant negative p53 fibroblasts. Cell lysates were extracted 12, 24 h after sham irradiation and 0, 3, 6, 9, 12, 24 h after 10 Gy irradiation. Bar graphs represent densitometric analyses of the p21 bands for the irradiated samples normalized to the respective 10 Gy irradiated 0 h p21 samples.

as compared to the empty vector control (Figure 1C), suggesting that SV40 immortalization does not completely eliminate p53 activity.

p53-dependent p21 induction and SV40 large T antigen expression. The p21 immunoblot experiments were repeated with the MRC-5 (primary) and MRC-

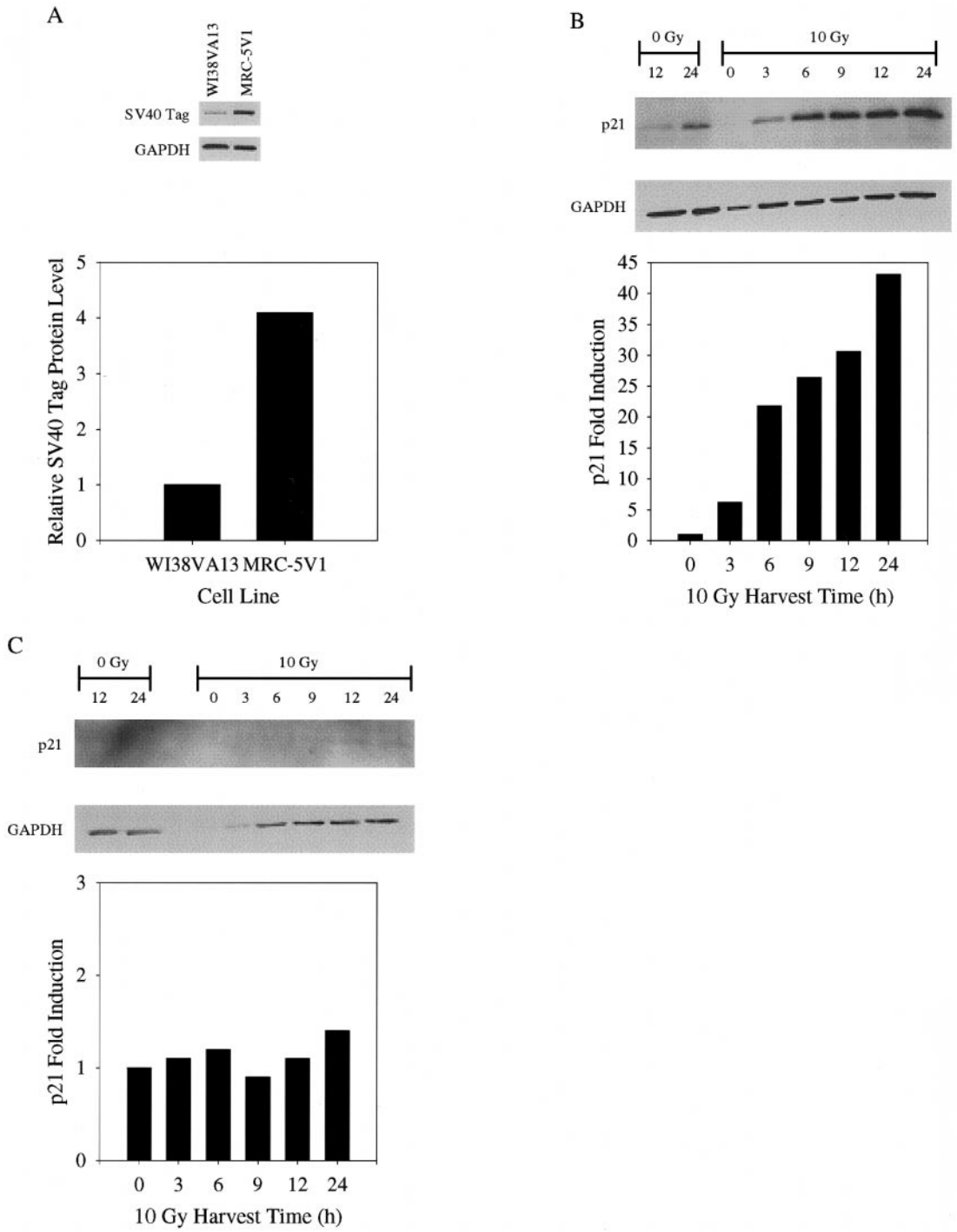

FIG. 2. Western blot analyses. A) Western blot showing expression of SV40 large T antigen in WI38VA13 and MRC-5V1 SV40 immortalized fibroblasts. Bar graph represents densitometric analysis of the SV40 Tag bands normalized to the WI38VA13 sample. Western blot showing p53-dependent p21 induction after 10 Gy ionizing radiation in B) MRC-5 and C) MRC-5V1 fibroblasts. Cell lysates were extracted 12, 24 h after sham irradiation and 0, 3, 6, 9, 12, 24 h after 10 Gy irradiation. Bar graphs represent densitometric analyses of the p21 bands for the irradiated samples normalized to the respective 10 Gy irradiated 0 h p21 samples.

5V1 (SV40 immortalized) cell lines to determine whether the degree of p21 inhibition was correlated with SV40 Tag expression, since MRC-5V1 cells have higher SV40 Tag levels compared to WI38VA13 (Figure 2A). The induction of p21 in MRC-5 was significant (Figure 2B), but was virtually eliminated in MRC-5V1

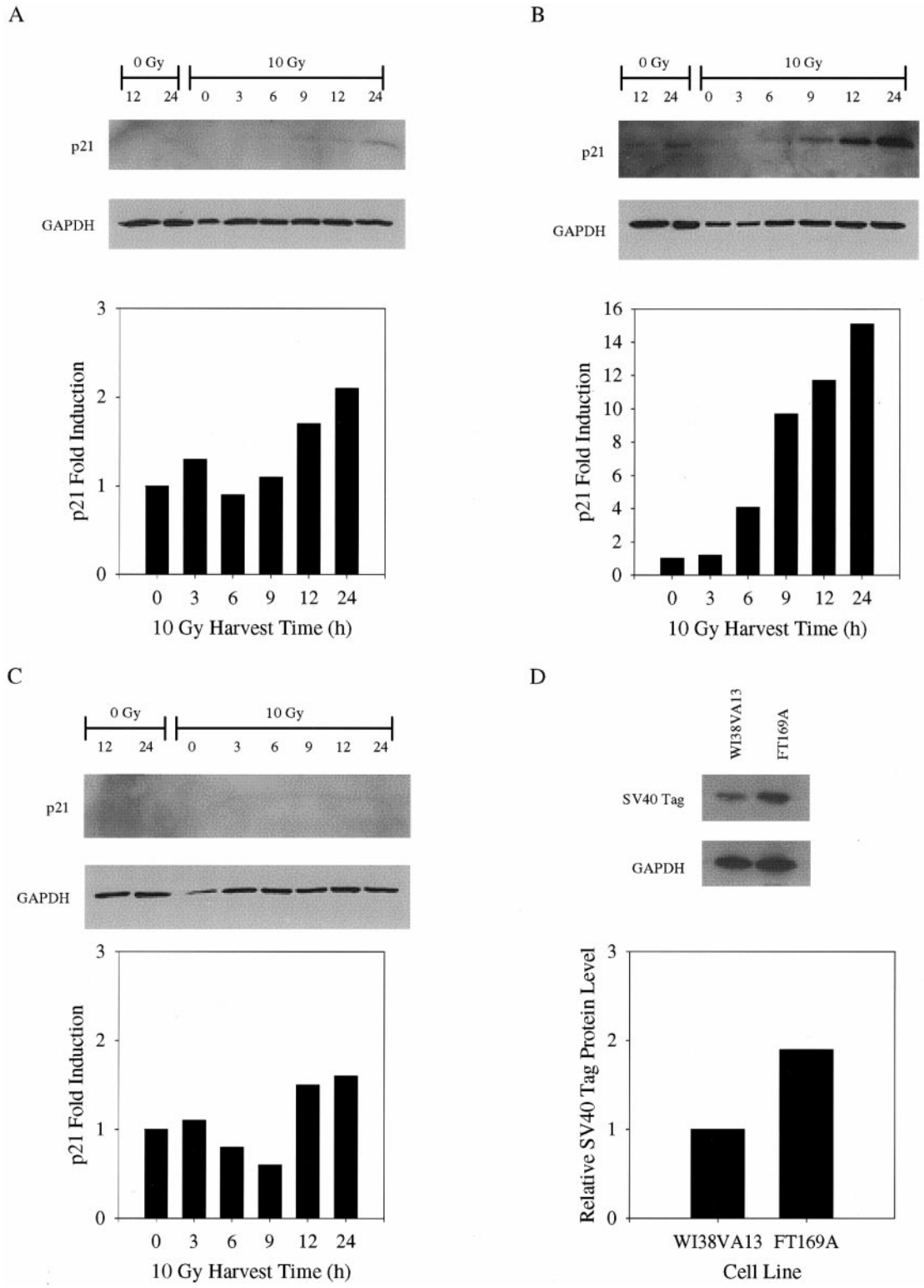

FIG. 3. Western blot analyses of FT169A A-T fibroblasts. Western blot showing p53-dependent p21 induction after 10 Gy ionizing radiation in A) FT169A pCMV-Neo-Bam empty vector, B) FT169A pC53-SN3 wild type p53, and C) FT169A pC53-SCX3 dominant negative p53 A-T fibroblasts. Cell lysates were extracted 12, 24 h after sham irradiation and 0, 3, 6, 9, 12, 24 h after 10 Gy irradiation. Bar graphs represent densitometric analyses of the p21 bands for the irradiated samples normalized to the respective 10 Gy irradiated 0 h p21 samples. D) Western blot showing expression of SV40 large T antigen in WI38VA13 and FT169A SV40 immortalized fibroblasts. Bar graph represents densitometric analysis of the SV40 Tag bands normalized to the WI38VA13 sample.

(Figure 2C), suggesting that the reduced p53 activity compared to WI38VA13 is probably due to increased p53 sequestration by SV40 Tag.

In order to confirm that p53 activity was being influenced by Tag expression, SV40 immortalized fibroblasts from a patient with the neurodegenerative disease A-T were used to assess p53 activity. A-T cells are known to have delayed induction of p53, and consequently a delayed induction of p21, in response to ionizing radiation (1, 15). Since the p53-dependent p21 response was already attentuated, we speculated that perhaps SV40 immortalization would further reduce p53 activity. FT169A cells transfected with the empty vector (pCMV-Neo-Bam) showed minimal p21 induction after 10 Gy ionizing radiation (Figure 3A). Whereas, overexpression of p53 in FT169A cells restored p53-dependent p21 induction with the delayed kinetics that is typical (Figure 3B), expression of dominant negative p53 removed p21 transactivation (Figure 3C). These findings again support the notion that the binding of p53 by SV40 Tag diminishes but does not completely abolish p53 dependent activity in SV40 immortalized cells.

Further evidence suggesting that p53 is still functional in SV40 immortalized fibroblasts is that overexpression of exogenous p53 in WI38VA13 resulted in cell death, while overexpression of p53 in FT169A fibroblasts, which harbor a higher level of SV40 Tag (Figure 3D), was not toxic. This suggested that perhaps overexpression of exogenous p53 in cells already harboring functional endogenous levels might exceed some toxic threshold.

SV40 immortalization and p53-dependent G_1 cell cycle arrest after irradiation. In order to assess p53 functionality at the phenotypic level, G_1 arrest was measured by flow cytometry to determine whether SV40 immortalization had any influence on the ability of p53 to arrest the cell cycle after DNA damage. Flow cytometry, following 10 Gy irradiation, was performed on the WI-38 and MRC-5 cell lines and their derivatives (Figure 4). The major indicators of G_1 arrest include the depletion of cells from early S phase and the retention of the G_1 peak in a standard flow cytometry histogram. Only the primary cells demonstrated G_1 arrest (Figures 4A and 4E). In all cases of SV40 immortalization, G_1 arrest was absent regardless of p53 status (Figures 4B, 4C, 4D, and 4F). The expression of dominant negative p53 (pC53-SCX3) in WI38VA13 did not alter the profile (Figure 4B vs. 4C), suggesting that the G_1 checkpoint inactivation in the WI38VA13 cell line was complete.

Since overexpression of wild-type p53 in FT169A A-T cells was not toxic, these cells were also assessed for G_1 arrest to determine whether the cell cycle checkpoint would be restored. As shown in Figure 5, G_1 arrest was completely absent in cells overexpressing p53 even

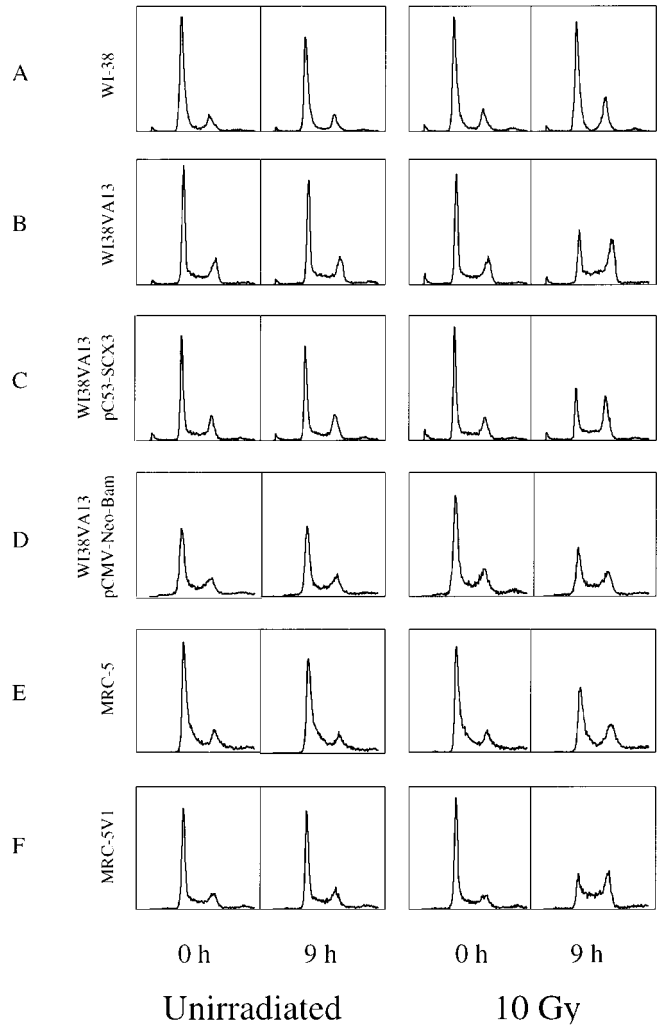

FIG. 4. Flow cytometry of A) WI-38, B) WI38VA13, C) WI38VA13 pC53-SCX3, D) WI38VA13 pCMV-Neo-Bam, E) MRC-5, and F) MRC-5V1 fibroblasts. In each set, first two histograms represent sham-irradiated samples harvested 0 and 9 h post-irradiation. Second two histograms represent 10 Gy irradiated samples harvested 0 and 9 h post-irradiation. All samples were fixed with 70% ethanol and stained with propidium iodide to plot cell number vs. DNA content.

though p21 transactivation was restored (Figure 3B). In addition, FT169A cells with dominant negative p53 had no G_1 arrest (Figure 5). Thus, SV40 immortalization appears to completely eliminate cell cycle checkpoint activity even when p53-dependent p21 transactivation is partially functional.

Radiation-induced apoptosis in SV40 immortalized human fibroblasts. Another significant p53-mediated phenotype is radiation-induced apoptosis. In order to determine whether p53 was functional in SV40 immortalized human fibroblasts, radiation-induced apoptosis was measured in both primary and SV40 immortalized cell lines, as well as the WI-38 p53 transfectants, to determine whether SV40 immortalization modulated

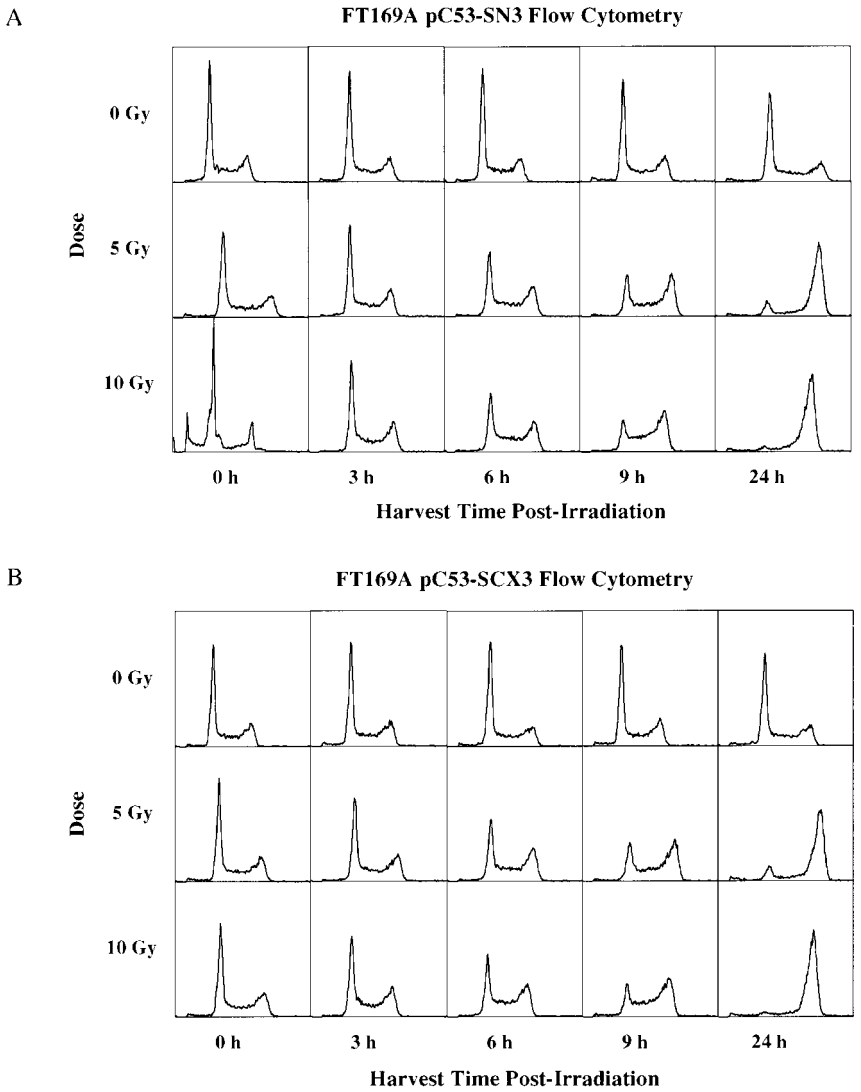

FIG. 5. Flow cytometry analysis of A) FTI169A pC53-SN3 and B) FT169A pC53-SCX3 A-T fibroblasts. Samples are either sham irradiated, 5 Gy irradiated, or 10 Gy irradiated and harvested 0, 3, 6, 9, 24 h post-irradiation and stained with propidium iodide to plot cell number vs. DNA content.

p53-dependent apoptosis. To address this issue, all cell lines were irradiated with 10 Gy gamma radiation and apoptosis was scored over 0, 24, 48, 72, and 96 h post-irradiation. Apoptosis was measured by counting cells that had the characteristic chromatin fragmentation as measured by DAPI (Figure 6A). As shown in Figure 6B, all SV40 immortalized cell lines, regardless of p53 status, had significantly increased apoptosis compared to the parental primary cell lines.

DISCUSSION

The SV40 Tag has been shown to bind to the tumor suppressor protein p53 (8–10). This binding activity ascribed to the large T antigen has been associated with its ability to transform primary murine cells (16, 17) and extend the lifespan of human cells (11). The p53-mediated response in SV40-transformed murine cells has recently been determined to be functional (12), but the DNA damage-induced p53 response in SV40-immortalized human cells has not been characterized. In this study, we have demonstrated, using three different SV40-immortalized cell lines, that the DNA damage-induced p53 response in SV40 immortalized human fibroblasts is partially functional with regard to radiation-induced p21 upregulation. However, radiation-induced G_1 arrest is completely absent in SV40 immortalized fibroblasts. In addition, SV40 immortalization upregulates radiation-induced apoptosis. Therefore, the data suggests that although resid-

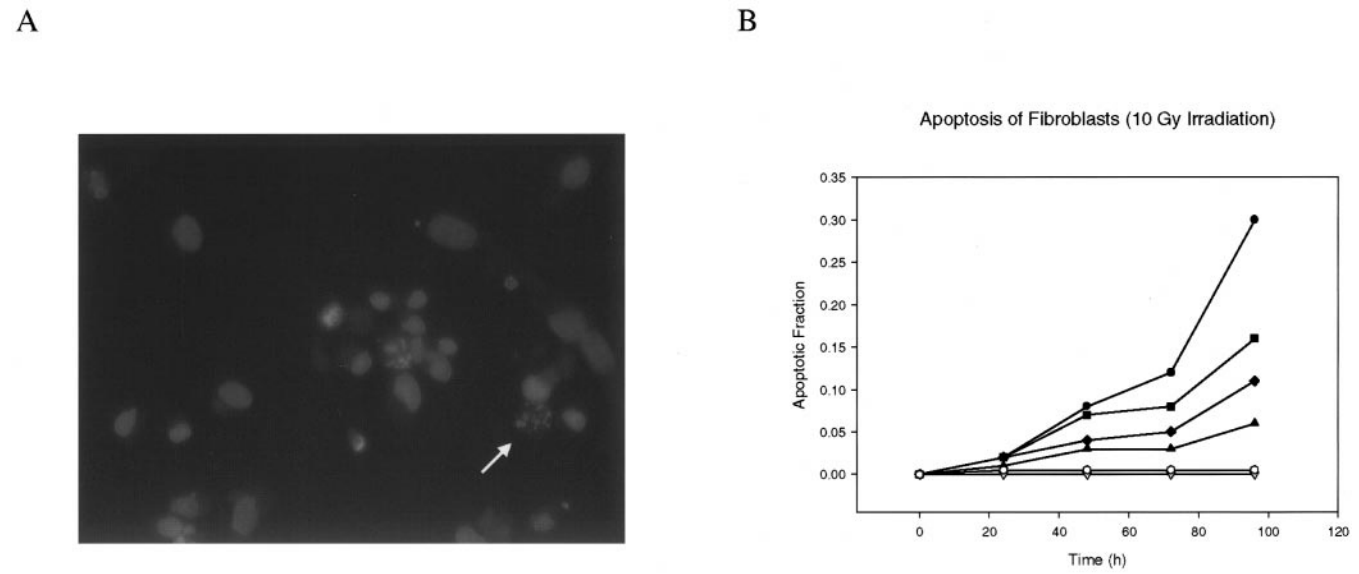

FIG. 6. Radiation-induced apoptosis of fibroblasts. A) Representative WI38VA13 apoptotic cell 96 h post-irradiation. DAPI stain. B) Plot showing apoptotic fraction of given cell lines measured 0, 24, 48, 72, and 96 h after 10 Gy ionizing radiation. Closed circle = MRC-5V1; closed square = WI38VA13; closed diamond = WI38VA13 pC53-SCX3; closed triangle = WI38VA13 pCMV-Neo-Bam; open hexagon = MRC-5; open inverted triangle = WI-38. MRC-5 plot has been artificially displaced from WI-38 plot for proper visualization. Data points represent the mean of two independent experiments.

ual p53 activity remains, SV40 immortalization engenders a new phenotype that can neither be classified as being p53-null nor as being wild-type for p53 activity.

The mechanism of this phenomenon needs to be elucidated, but at least three possibilities exist. First, the level of suppression of p53 activity by SV40 Tag may be enough to inhibit G_1 arrest but not apoptosis. In fact, the data suggest that although the characteristic kinetics of p53-mediated p21 transactivation are retained in SV40-immortalized cells, the magnitude of the response is reduced and G_1 arrest is absent. This suggests that a certain threshold of p21 activity may be required for G_1 arrest to occur post-irradiation. In WI38VA13, the residual p53 activity is sufficient for DNA damage-induced p21 transactivation, which can be further reduced through expression of dominant-negative p53. The attenuation of p21 transactivation is probably dependent upon the expression level of the SV40 Tag, since higher expression of SV40 Tag (e.g. MRC-5V1 fibroblasts) further attenuates p21 transactivation.

G_1 cell cycle arrest remained absent even when p53-dependent p21 transactivation was partially restored by overexpressing p53 in FT169A A-T fibroblasts. The restored p53-dependent p21 induction in FT169A cells was delayed as compared to primary fibroblasts, which is characteristic for A-T cells. Thus, overexpression of p53 in A-T cells restores characteristically delayed p21 expression in response to ionizing radiation.

In addition, the removal of p53 has traditionally been associated with decreased apoptosis (18). Despite the p53-null phenotype for G_1 arrest, all of the SV40-immortalized cells showed greatly increased apoptosis relative to primary cells. Recent evidence has suggested that merely the presence of some functional p53 is required for induction of apoptosis (19), so the p53 competent phenotype for apoptosis may reflect a lower activity threshold than for G_1 arrest. This explanation, however, is counterintuitive, since apoptosis is thought to be a consequence of excessive DNA damage, and G_1 arrest a protective measure against lower damage levels.

A second explanation for the presence of p53-mediated p21 transactivation and upregulated apoptosis without cell cycle arrest may be the fact that the amino terminus of SV40 Tag can also bind to Rb and Rb-related proteins (20), which are downstream of p53 and are directly responsible for inhibiting S phase initiation. This theory is consistent with earlier studies demonstrating that expression of the Rb-binding N-terminal domains of SV40 Tag was sufficient to overcome p53-mediated growth arrest in fibroblast cell lines (21, 22). Thus, Rb binding may be more significant than p53 binding in the inhibition of growth arrest by SV40 Tag.

Recent evidence has suggested that removal of cell cycle checkpoints upregulates apoptosis (23, 24). One may argue that the SV40 Tag-mediated loss of G_1 arrest through binding of Rb or a related mechanism may increase apoptosis post-irradiation because of a deregulated cell cycle checkpoint pathway. This hypothesis may be conceptually justified by considering that the failure of primary fibroblasts to undergo apoptosis may be due to their strong p21-induced G_1 arrest, since loss

of p21-mediated arrest results in increased apoptosis. In this model, then, all p53-dependent functions are actually normal in SV40 immortalized lines.

A third explanation for this phenomenon is that the SV40 Tag mediates radiation-induced apoptosis via a novel p53-independent mechanism that is yet to be described. The possibility that the SV40 Tag somehow is directly involved in the apoptotic response cannot be eliminated. However, there is no evidence to support this notion, and it would require that SV40 Tag stimulate a currently unknown damage-responsive transduction pathway.

These findings have wide-ranging implications, since many cellular studies, including molecular studies of genetic defects such as A-T, employ SV40 immortalized fibroblasts for mechanistic experimentation. Since SV40 immortalization apparently engenders a unique phenotype that is neither p53-null nor p53 wild-type, mechanistic conclusions about potentially p53-mediated responses are suspect, and care should be taken when drawing mechanistic conclusions about the involvement of p53.

ACKNOWLEDGMENTS

We gratefully acknowledge H. Tian and P. Russell for helpful discussions. This work was supported by Grant 9307-0016 from the National Aeronautics and Space Administration and P01-CA74175 from the National Cancer Institute of the National Institutes of Health, U.S. DHHS. Flow cytometry work was supported in part by the Lombardi Cancer Center Flow Cytometry/Cell Sorting Shared Resource, U.S. Public Health Service Grant 2P30-CA-51008.

REFERENCES

1. Kastan, M. B., Zhan, Q., El-Deiry, W. S., Carrier, F., Jacks, T., Walsh, W. V., Plunkett, B. S., Vogelstein, B., and Fornace, A. J., Jr. (1992) *Cell* **71,** 587–597.
2. El-Deiry, W. S., Tokino, T., Velculescu, V. E., Levy, D. B., Parsons, R., Trent, J. M., Lin, D., Mercer, W. E., Kinzler, K. W., and Vogelstein, B. (1993) *Cell* **75,** 817–825.
3. Bates, S., and Vousden, K. H. (1996) *Current Opinion in Genetics and Development* **6,** 12–18.
4. Siliciano, J. D., Canman, C. E., Taya, Y., Sakaguchi, K., Appella, E., and Kastan, M. B. (1997) *Genes Dev.* **11,** 3471–3481.
5. Hartwell, L. H., and Kastan, M. B. (1994) *Science* **266,** 1821–1828.
6. Pietenpol, J. A., Tokino, T., Thiagalingam, S., El-Deiry, W. S., Kinzler, K. W., and Vogelstein, B. (1994) *Proc. Natl. Acad. Sci. USA* **91,** 1998–2002.
7. Crook, T., Marston, N. J., Sara, E. A., and Vousden, K. H. (1994) *Cell* **79,** 817–827.
8. Lane, D. P., and Crawford, L. V. (1979) *Nature* **278,** 261–263.
9. Linzer, D. I. H., Maltzman, W., and Levine, A. J. (1979) *Cell* **17,** 43–52.
10. Sarnow, P., Ho, Y. S., Williams, J., and Levine, A. J. (1982) *Cell* **28,** 387–394.
11. Lin, J., and Simmons, D. T. (1991) *J. Virol.* **65,** 6447–6453.
12. Hess, R. D., and Brandner, G. (1997) *Oncogene* **15,** 2504.
13. Ziv, Y., Jaspers, N. G. J., Etkin, S., Danieli, T., Trakhtenbrot, L., Amiel, A., Ravia, Y., and Shiloh, Y. (1989) *Cancer Res.* **49,** 2495–2501.
14. Baker, S. J., Markowitz, S., Fearon, E. R., Willson, J. K. V., and Vogelstein, B. (1990) *Science* **249,** 912–915.
15. Khanna, K. K., and Lavin, M. F. (1993) *Oncogene* **8,** 3307–3312.
16. Zhu, J. Y., and Cole, C. N. (1989) *J. Virol.* **63,** 4777–4786.
17. Kierstead, T. D., and Tevethia, M. J. (1993) *J. Virol.* **67,** 1817–1829.
18. Westphal, C. H., Rowan, S., Schmaltz, C., Elson, A., Fisher, D. E., and Leder, P. (1997) *Nature Genet.* **16,** 397–401.
19. Barlow, C., Brown, K. D., Deng, C. X., Tagle, D. A., and Wynshaw-Boris, A. (1997) *Nature Genet.* **17,** 453–456.
20. DeCaprio, J. A., Ludlow, J. W., Frigge, J., Shew, J.-Y., Huang, C.-M., Lee, W.-H., Marsilio, E., Paucha, E., and Livingston, D. M. (1988) *Cell* **54,** 57–65.
21. Michael-Michalovitz, D., Yehiely, F., Gottlieb, E., and Oren, M. (1991) *J. Virol.* **65,** 4160–4168.
22. Quartin, R. S., Cole, C. N., Pipas, J. M., and Levine, A. J. (1995) *J. Virol.* **68,** 1334–1341.
23. Gorospe, M., Cirielli, C., Wang, X., Seth, P., Capogrossi, M. C., and Holbrook, N. J. (1997) *Oncogene* **14,** 929–935.
24. Waldman, T., Lengauer, C., Kinzler, K. W., and Vogelstein, B. (1996) *Nature* **381,** 713–716.